NOTES AND INSIGHTS

Surface Analysis Insight Note: Observations relating to photoemission peak shapes, oxidation state, and chemistry of titanium oxide films

Pascal Bargiela[1] | Vincent Fernandez[2] | William Ravisy[2] | David Morgan[3,4] | Mireille Richard-Plouet[2] | Neal Fairley[5] | Jonas Baltrusaitis[6]

[1]The Institute for Research on Catalysis and the Environment of Lyon (IRCELYON), Villeurbanne, France

[2]Nantes Université, CNRS, Institut des Matériaux Jean Rouxel de Nanites, IMN, Nantes, France

[3]Cardiff Catalysis Institute, Cardiff University, Cardiff, UK

[4]HarwellXPS—EPSRC National Facility for Photoelectron Spectroscopy, Research Complex at Harwell (RCaH), Didcot, Oxon, UK

[5]Casa Software Ltd, Teignmouth, Devon, UK

[6]Department of Chemical and Biomolecular Engineering, Lehigh University, Bethlehem, Pennsylvania, USA

Correspondence
Jonas Baltrusaitis, Department of Chemical and Biomolecular Engineering, Lehigh University, 111 Research Drive, Bethlehem, PA 18015, USA.
Email: job314@lehigh.edu

It is common practice to describe the coordination of metal atoms in a binding configuration with their nearest neighbors in terms of oxidation state, a measure by which the number of electrons redistributed between atoms forming chemical bonds. In XPS terms, change to an oxidation state is commonly inferred by correlating photoemission signal with binding energy. The assumption, when classifying photoemission signals into distinct spectral shapes, is that a distribution of intensities shifted to lower binding energy is evidence of a reduction in oxidation state. In this *Insight* note, we raise the prospect that changes in photoemission peak shape may occur without obvious changes, determined by XPS in stoichiometry for a material. It is well known that TiO_2 measured by XPS yields reproducible Ti 2p photoemission peaks. However, on exposing TiO_2 to ion beams, Ti 2p photoemission evolves to complex distributions in intensity, which are particularly difficult to analyze by traditional fitting of bell-shaped curves to these data. For these reasons, in this *Insight* note, a thin film of TiO_2 deposited on a silicon substrate is chosen for analysis by XPS and linear algebraic techniques. Alterations in spectral shapes created from modified TiO_2, which might be interpreted as the change in oxidation state, are assessed in terms of relative proportions of titanium to oxygen. It is found through detailed analysis of spectra that quantification by XPS, using procedures routinely used in practice, is not in accord with the typical interpretations of photoemission shapes. The data processing methods used and results presented in this work are of particular relevance to elucidating fundamental phenomena governing the surface evolution of materials-enabled energy processes where cyclic/non-steady usage changes the nature of bonding, especially in the presence of contaminants.

KEYWORDS
component spectra, linear least squares, oxidation state, titania, XPS

1 | INTRODUCTION

Quantification by XPS[1], for most users, means applying a set of steps prescribed by the manufacturers of the instrument used to collect their data. These steps necessarily involve the use of relative sensitivity factors (RSFs), some form of instrumental transmission correction[2], and, depending on RSFs, some form of explicit correction for the influence of escape depth on peak intensity. Both transmission and escape depth corrections are energy dependent, meaning the intensity of photoemission peaks is dependent on the energy at which the signal is recorded, while the escape depth also has a material dependency.[3] Quantification obtained by following the prescribed methodology is by no means perfect.[4] However, understanding why results from quantification fall short of the expected composition can be an important step in understanding a sample. When adjusting photoemission peak intensity to produce atomic concentration or peak ratios, two correction factors of concern are (1) the appropriateness of an escape depth correction and (2) the accuracy of the transmission correction. The former necessitates knowledge of the sample while the latter is dependent on the calibration of an instrument.[5] Because these two factors are energy dependent, their influence can be eliminated, to some extent, by selecting photoemission lines close in energy.

Controlled modification of the sample surface properties by external stimuli, such as temperature or ion beam, in general[6–9] and those of TiO_2 surfaces in particular,[10–14] has long been used to induce material property changes. In particular, these argon ion-beam exposure experiments and analyses create results for proposed reduced (Ti^{3+} or Ti^{2+}) chemical states which are typically associated and assigned to the corresponding crystalline titanium oxide materials, as implied by line shapes with peaks arising at the lower binding energy. The quantification, however, derived from photoemission intensities as shown in this *Insight*, does not necessarily support the assignment of reduced oxidation state compounds. The logic and analysis techniques are, therefore, presented below so that users of XPS are made aware of such anomalies in the interpretation of reducible metal oxide XPS data.

In this *Insight* note, we use a film of TiO_2 deposited using PECVD on a silicon substrate.[15] The TiO_2 is assumed to be more than three attenuation lengths in thickness, which is supported by the lack of silicon signal within spectra. Given the Ti 2p and O 1s photoemission lines are close in energy (∼70 eV separation), we can use these two signals to determine the relative proportions of titanium and oxygen within the film without significant errors due to transmission, but more importantly, their use reduces errors due to escape depth, the influence of which alters with film thickness. The results, presented in this work, make use of linear algebra to construct, from data, component spectra with shapes characteristic of different phases of the sample throughout the experiment. These component spectra are quantified and shown to yield spectroscopic shapes that would suggest an altered oxidation state but relative intensities of photoemission peaks that suggest little change in stoichiometry. The question of the suitability of line shapes derived by the linear algebra is assessed by a challenge study performed by extracting the line shapes

computed for Ti 2p only and applying these computed shapes to data from a second experiment conducted in a different regime from the experiment used to compute the line shapes. The second experiment involved measuring spectra along a line scan of stage movements over a surface exposed to the ion beam. Variation in spectral shapes, in this second experiment, is due to variation in ion-beam flux over the large area affected.

2 | EXPERIMENTAL

Sample analysis was performed using a Kratos Axis NOVA X-ray photoelectron spectrometer with a Minibeam 4 ion source. The base pressure in the analysis chamber was 4×10^{-10} Torr without X-ray and 1×10^{-9} Torr and 3.3×10^{-8} Torr with X-rays and during argon ion sputtering, respectively. A monochromatic source (300 W) was used with the analysis acquired from the 300×700 μm surface area with a pass energy of 20 eV and energy step of 0.1 eV. Under these conditions, Ag Fermi edge resolution is 0.4 eV. The measurements were performed without using a charge neutralizer. High energy regions of O 1s Ti 2p, N 1s, C 1s Ti 3p O 2s, and valence band were acquired. Before ion sputtering experiments, the gas line was purged three times. Ions are created at 2000 eV and decelerated to 500 eV. The sputtered surface area was about 8×8 mm.

The method used to modify TiO_2 from the initial well-formed Ti^{4+} material is to irradiate the surface with a single-spot beam of low-energy monoatomic argon ions of 500 eV defocused to spread over a large area. The rate of change in spectral shapes, as measured by Ti 2p, is controlled by the time that the sample is exposed to the ion beam between XPS measurements. The experiment is performed in three stages. Initially, sputtering for 10 s between XPS cycles continued until the evolution in Ti 2p converged to a relatively constant line shape. The sputter time was then increased to 50 s per sputter cycle. The final stage of the experiment involved sputtering for 250 s per sputter cycle. Extending the sputter time produces new shapes in the Ti 2p spectra, not apparent for data collected following 10 s per sputter cycle.

All data were analyzed using CasaXPS version 2.3.25PR1.0.27.[16] The analysis of these data makes use of linear algebraic methods and traditional nonlinear least squares fitting of peak models to data.[17] Quantification of photoemission signal is performed using the method prescribed by Kratos Analytical Ltd for data recorded on Axis Nova XPS instruments. Quantification of the sample in terms of titanium, oxygen, and carbon was performed using integration regions, in which signal above a Shirley background[18] was corrected for relative sensitivity and transmission. Quantification by these means assumes a bulk homogeneous sample, which in the absence of adventitious material is valid for the TiO_2 sample used herein. Controlled changes to these Ti 2p spectra are a prerequisite for the analysis of data using linear algebra.[6,8] The stability of the spectra (concerning energy) during XPS and sputtering cycles is also a requirement for the analysis of these data. Thus, at each increment in time per sputter cycle, a repeat measurement was performed to ensure at each stage in the experiment

the spectra, in the absence of ion-beam intervention, were reproducible. These checks are important because, when spectra such as Ti 2p are observed to alter in shape, the possibility of charging effects as electrons are emitted from the sample and ions with opposite charges impact the surface may distort spectra between measurements.[19,20] Central to the analysis of these Ti 2p spectra is the acquisition of O 1s, C 1s, Ti 3p, O 2s, and valence band spectra. Ti 2p, O 1s, and C 1s were of importance because peak models fitted to O 1s and C 1s provided necessary information when interpreting elemental quantification. These three narrow scan spectra also served to support the assertion that charging effects in spectra were not significant to the analysis described below. Namely, evolution in the Ti 2p spectra manifested as a signal moving to lower binding energy, while the O 1s signal was relatively stable in shape with small changes predominantly to higher binding energy and C 1s attenuated in intensity but appeared to have a consistent binding energy. Ti 3p, O 2s, and valence band were also included in the analysis resulting in the component spectra characteristic of different phases of TiO_2. These observations all contribute to the belief that these changes in Ti 2p spectra genuinely reflect changes in the sample and are without significant instrumental artifacts.

3 | RESULTS AND DISCUSSION

When measured from a pure TiO_2 material in a 4+ oxidation state, the characteristic of Ti 2p is among the simplest photoemission from metal oxides. This statement is borne out in the Ti 2p spectra shown in Figure 1A. The spectrum corresponding to the as-received surface is typical of Ti^{4+}, where photoemission results in two well-resolved peaks, possessing line shapes with Voigt characteristics.[21] There is little evidence of overlapping satellite structures often seen in other d-block metal oxide spectra,[22–24] suggesting that photo-ionization of titanium in the 4+ oxidation state is well-defined in both the initial and final state for the atom in the solid state. However, the contrast between Ti 2p spectra before and after exposure to ion-beam sputtering is significant. Figure 1 shows a sequence of spectra measured from TiO_2 film deposited on a silicon substrate where an ion beam has been used to modify the surface. Argon ions of energy 500 eV spread over a large area alter the surface properties, creating obvious changes to photoemission peaks, but for which shape changes in Ti 2p data are the most apparent. Following sputtering with an ion beam, the core-level peaks for 4+ titanium gain shoulders of intensity to lower binding energy of the initial Ti 2p doublet (Figure 1A). The magnitude of these shoulders increases with each ion-beam cycle and the extent of these lower binding energy features continues to spread in energy the longer the sample is exposed to the ion beam. Presented with evidence of this form, the assumption for most samples analyzed by XPS is these changes to the shape of a photoemission peak represent changes in stoichiometry between atoms in the sample. However, in the case of titanium, these changes in photoemission peak shape do not easily conform to this model of photoemission. Changes to Ti 2p peak shape are clear in Figure 1A, but the ratio of titanium to oxygen

does not support the assumption that these photoemission peak shapes correspond to different stoichiometry. Data shown in Figure 1A–C were used to monitor changes in elemental composition with time of the sample exposed to the ion beam. The profile plot in Figure 1E quantifies these changes in the relative proportions of elements identified in the sample. The point to observe is how the ratio of titanium to oxygen varies initially over measurement cycles for which carbon is a significant proportion of the atomic concentration. Then, following the change from 10 s per sputter cycle to 50 s per sputter cycle, the ratio of titanium to oxygen plateaus in the Ti:O ratio equal to 1:2. Reduction of titanium would imply changes to the ratio of titanium to oxygen, which Figure 1 does not support.

The question following inspection of Figure 1E is if the reduction in titanium has occurred, how is it possible that oxygen is retained in the sample following the breaking and forming of bonds with titanium? The element in the analysis chamber during any XPS experiment but not open to detection is hydrogen. The other element other than titanium capable of bonding with oxygen is carbon. There is little evidence in the C 1s spectra that oxygen bonded to carbon increases with sputter time, but the role played by hydrogen is difficult to assess by XPS. The only means of making a judgment about hydrogen is to analyze the oxygen signal, which can be seen in Figure 1B (O 1s) and Figure 1D (O 2s). Both O 1s and O 2s undergo little change by sputtering, so changes due to altered carbon/oxygen chemistry or hydrogen/oxygen chemistry are difficult to assess by fitting synthetic line shapes to the highly correlated data in Figure 1B. Fortunately, carbon/oxygen chemistry is available through changes to C 1s spectra (Figure 1C), which can be seen to diminish with sputter time. It is reasonable to assume hydrogen/oxygen chemistry would similarly diminish with sputter time.

The most common approach, when presented with data of the form in Figure 1A, is to fit sets of doublet synthetic peaks to spectra, which are modeled by Voigt line shapes. Each pair of synthetic peaks is interpreted as a different oxidation state of titanium. However, the data in Figure 1 are of a form suitable for an alternative analysis that makes use of all photoemission lines to compute, from data, extended line shapes to correlate photoemission from different elements. The advantage to this alternative approach is interpretations for changes that occur in Ti 2p can be viewed in the context of other photoemission lines. Therefore, rather than attempting to construct peak models using synthetic line shapes fitted by nonlinear least squares optimization, spectra in Figure 1 are transformed into spectroscopic shapes using an approach that is now described.

Changes in Ti 2p spectra in Figure 1A are characterized by analysis techniques in CasaXPS[16] involving principal component analysis (PCA), linear algebraic manipulation of spectra (LAMS), and linear least squares (LLS) optimization.[25] The output from PCA is the number of distinct vectors (abstract factors [AFs]) required to properly describe all spectra shown in Figure 1, and as a by-product of identifying vectors of most significance to these data, data smoothing is achieved. Using only PCA AFs deemed to be significant, performing LLS fitting of these significant PCA AFs to data eliminates a proportion of noise from spectra.[6,8] These smoothed spectra are the input to LAMS. The
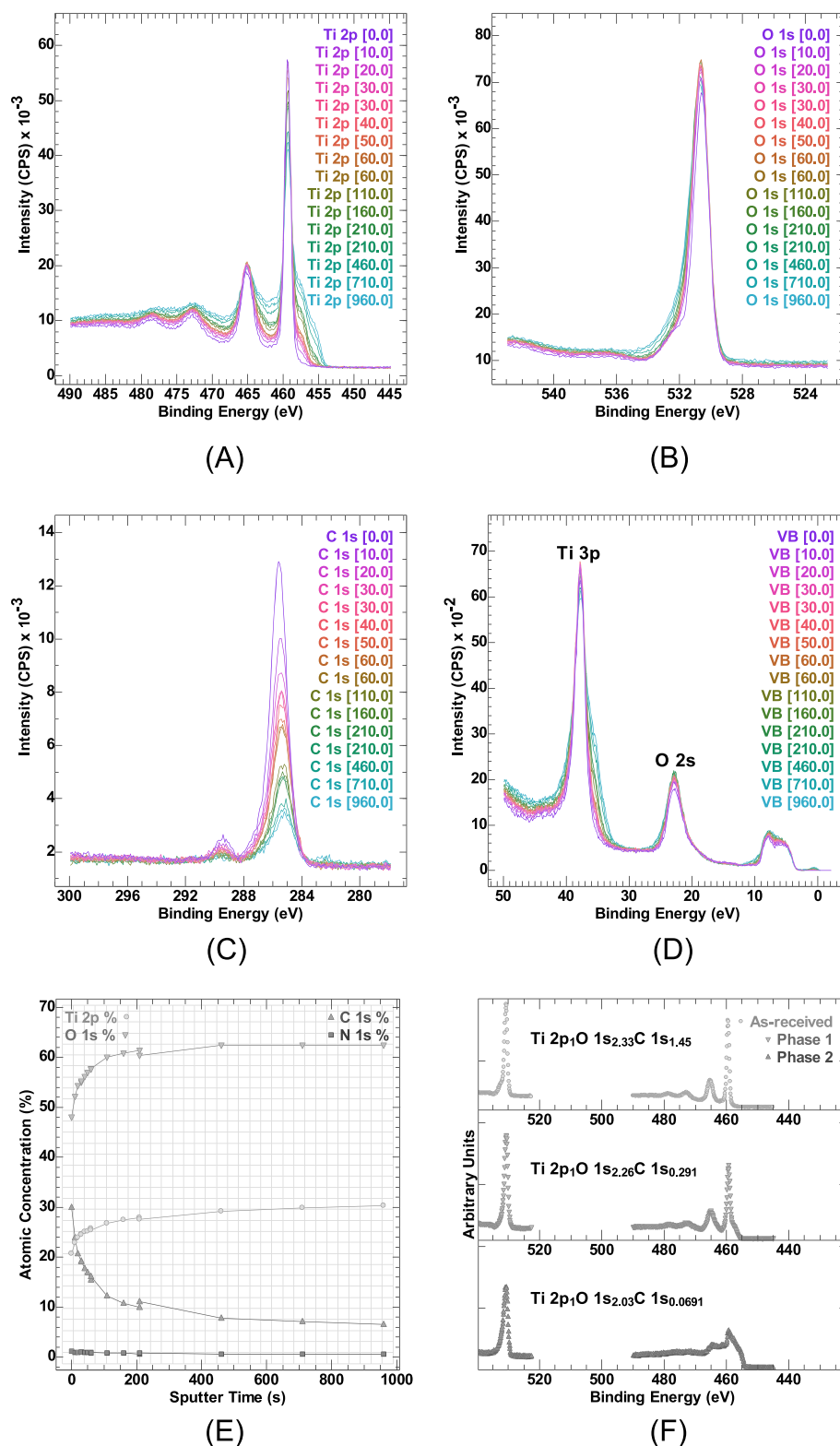
FIGURE 1 Spectra from a TiO$_2$ film on a Si wafer where XPS narrow scan spectra are collected following sputter cycles using 500 eV argon ions. Evolution of (A) Ti 2p; (B) O 1s; (C) C 1s; and (D) Ti 3p, O 2s, and valence band spectra induced by the ion beam. (E) Profile of atomic concentration versus sputter time. (F) Spectral component spectra computed by principal component analysis (PCA) and linear algebraic manipulation of spectra (LAMS) using CasaXPS.[16] Proportions of titanium, oxygen, and carbon are computed from the corresponding Ti 2p, O 1s, and C 1s spectral shapes within these component spectra.

process of converting spectra in Figure 1 to component spectra shown in Figure 1F is achieved by LAMS. LAMS is performed on vectors constructed from spectra, where each vector is the merged set of intensities and data bins available from Ti 2p, O 1s, C 1s, Ti 3p, O 2s, and valence band spectra shown in Figure 1. LAMS involves selecting vectors constructed by these means, on a pairwise basis. For each pair

of spectra, new spectral forms are constructed by subtracting one from the other in different proportions. These new spectral shapes are searched, looking for spectral shapes that offer insight into material properties. Figure 1F displays three spectral forms that emerge from an analysis of the data in Figure 1. These spectral forms are used to reconstruct data by LLS fitting these semiempirical spectral shapes

to the raw data. Thus, these computed spectral forms are the input to the LLS calculation that ultimately allows the partitioning of spectra into different phases induced by sputtering TiO_2. Hence, once computed, the selected spectral forms are better described as component spectra to a model to which LLS fitting is applied. Component spectra are chosen to maintain physically acceptable shapes for all photoemission lines. Following iterations of these LAMS steps, component spectra (Figure 1F) are computed which are used to assess changes within spectra due to sputtering of TiO_2 by argon ions.

The component spectra in Figure 1F are displayed with text strings indicating the relative proportions for titanium, oxygen and carbon in the format Ti $2p_1$O $1s_x$C $1s_y$, where the subscripts x and y are the ratio of oxygen and carbon concerning the amount of titanium. These results, calculated for each component spectrum, suggest there is an excess of oxygen relative to titanium in the first two component spectra labeled *as-received* and *phase 1*. However, in both component spectra, a carbon signal is also present, providing a possible explanation for the excess of oxygen in the form of carbon bonded to oxygen. A key point to observe is the classical Ti 2p doublet shape is available in the *as-received* component spectrum, yet the component spectrum labeled *phase 1* includes a signal to the lower binding energy of the *as-received* component spectrum but without any statistically significant change in the proportions of titanium and oxygen. Further, the component spectrum labeled *phase 2*, by contrast, does not include any carbon signal, is significantly changed in shape from the *as-received* component spectrum, but yields a ratio for titanium to oxygen of 1:2. Because these component spectra fit all spectra with similar success, the partitioning of raw data into this component spectra is possible and all three component spectra appear to yield the ratio of titanium to oxygen with stoichiometry 1:2 expected for Ti^{4+}. Given that the sputter experiment appeared to create two obvious shifts to lower binding energy for Ti 2p, the expectation is at least two different oxidation states were created. Thus, the exact nature of the surface following sputtering does not appear to follow the norms for XPS data analysis.

When confronted with anomalies of this nature, the first question to ask is how reproducible are these results. Therefore, a second experiment was performed to create Ti 2p spectra with similar evolution in shape but obtained by a single use of the ion beam that served two purposes: first, to test the component spectra with spectra acquired under a different regime and second, to measure the size of the ion-beam spot on the sample. Results from these analysis steps
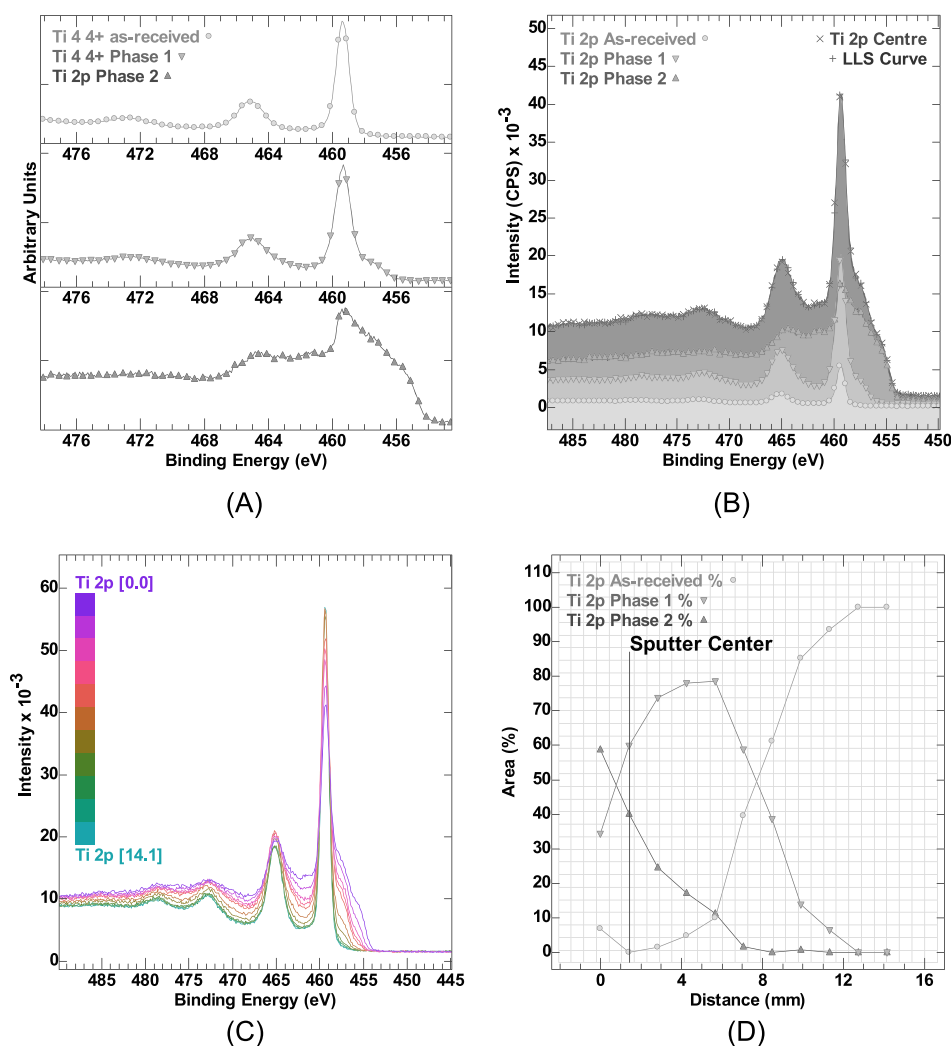

FIGURE 2 Ti 2p spectra collected along a stage-movement line scan of analysis positions fitted with three Ti 2p component spectra, the shape of which is constructed using data in Figure 1. (A) Ti 2p component spectra constructed by analysis of data described in Figure 1. (B) An example of a fit of the component spectra in (A) to a spectrum selected from Ti 2p spectra shown in (C). (C) Ti 2p spectra showing the evolution in Ti 2p shape because of changing analysis position along a line from the middle of the sputter-affected sample to locations where the influence of the ion beam is minimal. (D) Line scans calculated from peak areas of different phases, characterized by the component spectra in (A), of the sample stimulated by ion-beam sputtering.

for Ti 2p component spectra are shown in Figure 2A,B. This second data set is formed by sputtering the sample to prepare a modified surface where the sample at different points is affected to differing degrees determined by variation in ion-beam flux as a function of distance from the ion-beam center. A range of photoemission Ti 2p line shape results (Figure 2C) where the greatest change from the as-received surface Ti 2p spectrum occurs at the central position. A line scan of XPS data ranging from the central location to a point where the Ti 2p spectra return to a shape characteristic of the as-received sample was performed and resulted in a sequence of spectra
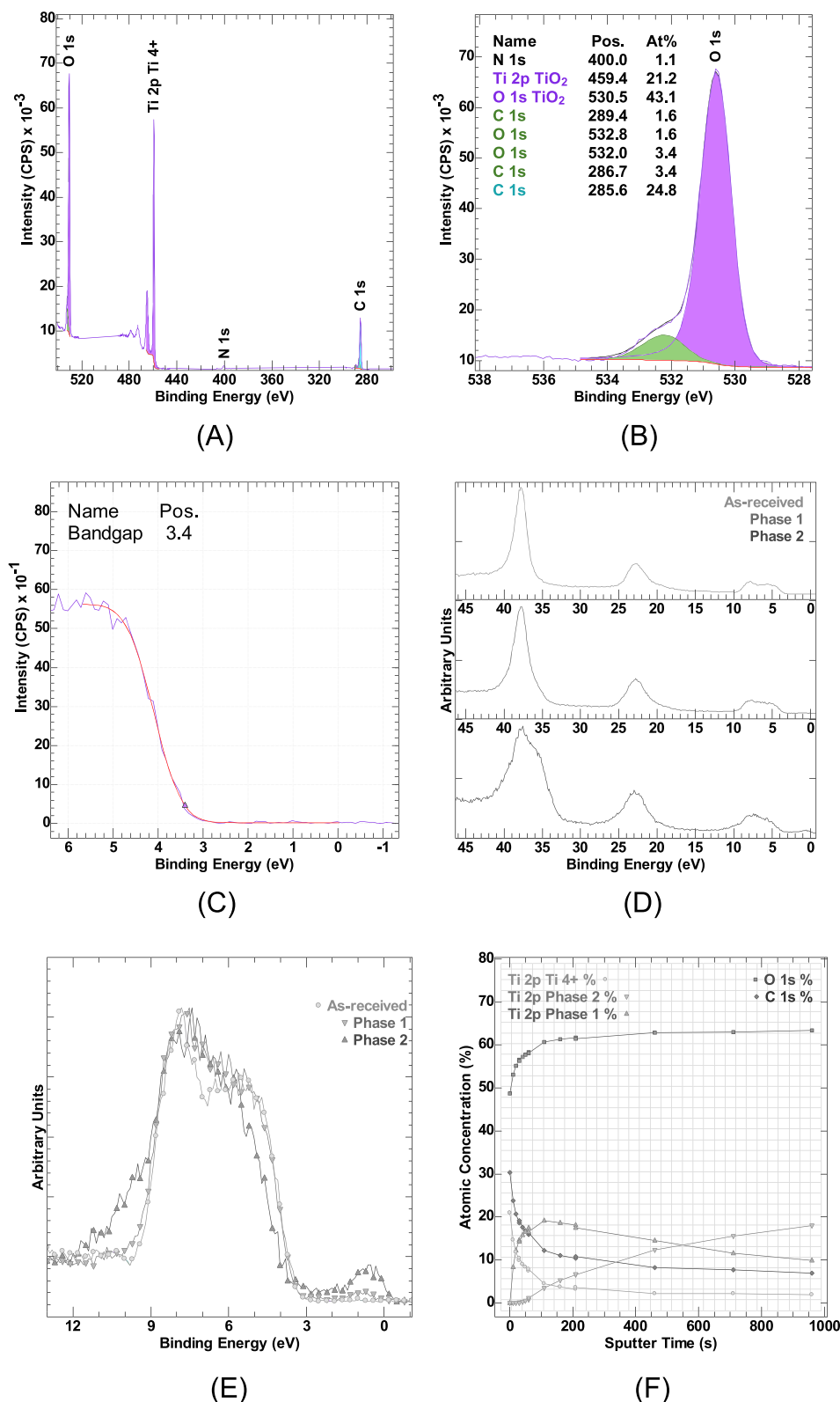

FIGURE 3 Quantification of the as-received sample demonstrates, through the fitting of components, the feasibility of the TiO$_2$ assignment. (A) Narrow scan spectra merged to form vectors corresponding to O 1s, Ti 2p, N 1s, C 1s, and valence band (shown in (C)). (B) O 1s narrow scan spectrum corresponding to data shown in (A) fitted with Voigt line shapes. The quantification table specifically illustrates that the oxygen signal can be correlated with the carbon signal, which, once the O 1s signal is correlated with the Ti 2p signal, the expected 2:1 stoichiometry for O:Ti in TiO$_2$ is recovered. (C) Valence band data corresponding to data in (A) illustrates that the onset of the signal associated with band structures in the as-received sample is compatible with titanium in a 4+ oxidation state. (D) Ti 3p, O 2s, and valence band component spectra correspond to deeper core-level photoemission shown in Figure 1F. (E) Valence band spectra corresponding to the component spectra are shown in Figure 1F. (F) Profile of sample changes induced by sputtering equivalent to the profile in Figure 1E, where the three phases of titanium are separated to show the dependence of phase creation on sputter time. Initially, the sputter cycles were of a duration of 10 s, during which phase 2 changes did not occur. Only when the sputter time is increased to 50 s per sputter cycle does phase 2 begin to change. Increasing the sputtering time to 250 s per sputter cycle serves to continue the trend of increasing phase 2 contributions to spectra.

analogous to the spectra in Figure 1A. An analysis of these Ti 2p spectra generated along a line scan is performed by extracting, from the component spectra computed using data in Figure 1, the shapes derived for Ti 2p only. These Ti 2p component spectra are shown in Figure 2A. An example of fitting a specific Ti 2p spectrum from the line scan is shown in Figure 2B. Applying fits data of the form shown in Figure 2B to all Ti 2p spectra (Figure 2C) collected along the line scan yields the line scan of the relative peak area shown in Figure 2D, where the evolution in Ti 2p spectra as a function of position on the sample is characterized in terms of three spectral shapes for Ti 2p. The point of demonstrating the use of component spectra calculated from data in Figure 1, applied to data in Figure 2 is that, these shapes for Ti 2p are reproducible.

Further evidence suggesting the as-received sample is compatible with a material in which titanium appears in a 4+ oxidation state is presented in Figure 3. The quantification for the same component spectra shown in Figure 1F suggests the O:Ti ratio is 2.3:1, but an analysis of the same data using Voigt line shapes to partition oxygen signal associated with titanium, from oxygen signal that predominantly is associated with carbon, demonstrates that the ratio for O:Ti in the as-received sample is better described as 2:1. Similarly, the valence band signal is offset by 3.4 eV relative to the Fermi edge for titanium metal (Figure 3C), an observation that is also compatible with titanium in a 4+ oxidation state. Thus, the component spectrum labeled phase 2 in Figure 1F, when compared through stoichiometry, is equivalent to the as-received sample before sputtering with an ion beam. Figure 3D does suggest signal for phase 2 is found within the band gap of TiO_2, which often is interpreted as the change in chemistry. Figure 3E compares the band spectra revealed by these three component spectra in more detail. While the band structure corresponding to phase 2 is different from the as-received TiO_2 film, the question remains whether the additional signal within the bandgap of TiO_2 is evidence of changes to bonds between titanium and oxygen, or whether such changes are due to altered physical properties of the film. The latter explanation would be consistent with the observation that stoichiometry between titanium and oxygen does not change between these three examples of component spectra. The two obvious differences highlighted by XPS are that carbon is removed and atoms have been in contact with argon ions. In this sense, these three component spectra are a product of the intervention by the ion beam. However, it has been reported previously that partial reduction of materials containing Ti^{4+} can be achieved by irradiation with UV light.[26] Thus, a less invasive modification to Ti^{4+} results in changes to the photoemission of Ti 2p and valence band signal, and does so by creating spectroscopic features similar in shape to phase 1. It should be noted that to achieve changes to the sample leading to spectra for which the phase 2 component spectrum is important, the required sputter cycle times 25 times longer than was required to create phase 1-type shapes in spectra (Figure 3F). Based on this evidence, it would be difficult to conclude that the evolution in the shape of photoemission from titanium illustrated in Figures 1 and 3F is due entirely to changes in sample oxidation states but rather is due to chemistry

associated with geometric and spatial alterations between titanium and oxygen.

4 | CONCLUSIONS

An example is presented, where evolution in core-level peak shapes seems to imply a reduction in oxidation state; however, this is found to be at odds with quantitative analysis for the said material. The evidence presented for XPS of a TiO_2 film on silicon suggests that changes in structures apparent in photoemission peaks, while reflecting alteration to sample properties, do not always imply changes in stoichiometry for a material. Ion beams may induce many-body effects as recently outlined by Bagus and coworkers. In particular, Bagus scrutinized Ti $2p_{1/2}$ peak broadening and concluded that it is due to the core-hole state mixing with the shake-up configurations resulting in Ti $2p_{1/2}$ core hole mixing with the Ti $2p_{3/2}$ core hole.[27] Another possibility is that ion beams may induce surface defects that are known to act as electron scavengers[28] resulting in spatially inhomogeneous electron distribution, an example of the phenomena observed in this work.

AUTHOR CONTRIBUTIONS

Pascal Bargiela: Investigation; writing—review and editing. **Vincent Fernandez:** Investigation; writing—review and editing. **William Ravisy:** Investigation. **David Morgan:** Investigation; writing—review and editing. **Mireille Richard-Plouet:** Writing—review and editing. **Neal Fairley:** Conceptualization; investigation; methodology; writing—original draft; writing—review and editing. **Jonas Baltrusaitis:** Conceptualization; investigation; methodology; supervision; writing—original draft; writing—review and editing.

CONFLICT OF INTEREST STATEMENT

The authors declare no competing interests.

DATA AVAILABILITY STATEMENT

Data are available on request from the authors.

ORCID

David Morgan https://orcid.org/0000-0002-6571-5731
Jonas Baltrusaitis https://orcid.org/0000-0001-5634-955X

REFERENCES

1. Shard AG. Practical guides for x-ray photoelectron spectroscopy: quantitative XPS. *J Vac Sci Technol A*. 2020;38(4):041201. doi:10.1116/1.5141395

2. Cumpson PJ, Seah MP, Spencer SJ. The calibration of Auger and X-ray photoelectron spectrometers for valid analytical measurements. *Spectrosc Eur*. 1998;10(3):8-15.

3. Seah MP. Simple universal curve for the energy-dependent electron attenuation length for all materials. *Surf Interface Anal*. 2012;44(10):1353-1359. doi:10.1002/sia.5033

4. Reed BP, Cant DJH, Spencer SJ, et al. Versailles Project on Advanced Materials and Standards interlaboratory study on intensity calibration for x-ray photoelectron spectroscopy instruments using low-density polyethylene. *J Vac Sci Technol A*. 2020;38(6):063208. doi:10.1116/6.0000577

5. Shard AG, Counsell JDP, Cant DJH, et al. Intensity calibration and sensitivity factors for XPS instruments with monochromatic Ag Lα and Al Kα sources. *Surf Interface Anal*. 2019;51(7):763-773. doi:10.1002/sia.6647

6. Fernandez V, Morgan D, Bargiela P, Fairley N, Baltrusaitis J. Combining PCA and nonlinear fitting of peak models to re-evaluate C 1s XPS spectrum of cellulose. *Appl Surf Sci*. 2023;614:156182. doi:10.1016/j.apsusc.2022.156182

7. Baltrusaitis J, Mendoza-Sanchez B, Fernandez V, et al. Generalized molybdenum oxide surface chemical state XPS determination via informed amorphous sample model. *Appl Surf Sci*. 2015;326:151-161. doi:10.1016/j.apsusc.2014.11.077

8. Garland BM, Fairley N, Strandwitz NC, Thorpe R, Bargiela P, Baltrusaitis J. A study of in situ reduction of MoO_3 to MoO_2 by X-ray photoelectron spectroscopy. *Appl Surf Sci*. 2022;598:153827. doi:10.1016/j.apsusc.2022.153827

9. Fairley N, Bargiela P, Huang W-M, Baltrusaitis J. Principal component analysis (PCA) unravels spectral components present in XPS spectra of complex oxide films on iron foil. *Appl Surf Sci Adv*. 2023;17:100447. doi:10.1016/j.apsadv.2023.100447

10. Majhi R, Rajbhar MK, Das P, Elliman RG, Chatterjee S. Low energy ion beam-induced joining of TiO_2 nanoparticles. *J Alloys Compd*. 2022;924:166440. doi:10.1016/j.jallcom.2022.166440

11. Sumita T, Otsuka H, Kubota H, et al. Ion-beam modification of TiO_2 film to multilayered photocatalyst. *Nucl Instrum Methods Phys Res Sect B Beam Interact Mater Atoms*. 1999;148(1–4):758-761. doi:10.1016/S0168-583X(98)00809-X

12. Takeuchi M, Onozaki Y, Matsumura Y, Uchida H, Kuji T. Photoinduced hydrophilicity of TiO_2 thin film modified by Ar ion beam irradiation. *Nucl Instrum Methods Phys Res Sect B Beam Interact Mater Atoms*. 2003;206:259-263.

13. Jackman MJ, Thomas AG, Muryn C. Photoelectron spectroscopy study of stoichiometric and reduced anatase TiO_2 (101) surfaces: the effect of subsurface defects on water adsorption at near-ambient pressures. *J Phys Chem C*. 2015;119(24):13682-13690. doi:10.1021/acs.jpcc.5b02732

14. Srivastava S, Thomas JP, Rahman MA, et al. Size-selected TiO_2 nanocluster catalysts for efficient photoelectrochemical water splitting. *ACS Nano*. 2014;8(11):11891-11898. doi:10.1021/nn505705a

15. Ravisy W, Richard-Plouet M, Dey B, et al. Unveiling a critical thickness in photocatalytic TiO_2 thin films grown by plasma-enhanced chemical vapor deposition using real time in situ spectroscopic ellipsometry. *J Phys D Appl Phys*. 2021;54(44):445303. doi:10.1088/1361-6463/ac1ec1

16. Fairley N, Fernandez V, Richard-Plouet M, et al. Systematic and collaborative approach to problem solving using X-ray photoelectron spectroscopy. *Appl Surf Sci Adv*. 2021;5:100112. doi:10.1016/j.apsadv.2021.100112

17. Major GH, Fernandez V, Fairley N, Smith EF, Linford MR. Guide to XPS data analysis: applying appropriate constraints to synthetic peaks in XPS peak fitting. *J Vac Sci Technol A*. 2022;40(6):063201. doi:10.1116/6.0001975

18. Shirley DA. High-resolution X-ray photoemission spectrum of the valence bands of gold. *Phys Rev B*. 1972;5(12):4709-4714. doi:10.1103/PhysRevB.5.4709

19. Béchu S, Richard-Plouet M, Fernandez V, Walton J, Fairley N. Developments in numerical treatments for large data sets of XPS images. *Surf Interface Anal*. 2016;48(5):301-309. doi:10.1002/sia.5970

20. Bargiela P, Fernandez V, Cardinaud C, et al. Towards a reliable assessment of charging effects during surface analysis: accurate spectral shapes of ZrO_2 and Pd/ZrO_2 via X-ray photoelectron spectroscopy. *Appl Surf Sci*. 2021;566:150728. doi:10.1016/j.apsusc.2021.150728

21. Major GH, Fairley N, Sherwood PMA, et al. Practical guide for curve fitting in x-ray photoelectron spectroscopy. *J Vac Sci Technol A*. 2020;38(6):061203. doi:10.1116/6.0000377

22. Morgan DJ. Resolving ruthenium: XPS studies of common ruthenium materials. *Surf Interface Anal*. 2015;47(11):1072-1079. doi:10.1002/sia.5852

23. Scanlon DO, Watson GW, Payne DJ, Atkinson GR, Egdell RG, Law DSL. Theoretical and experimental study of the electronic structures of MoO_3 and MoO_2. *J Phys Chem C*. 2010;114(10):4636-4645. doi:10.1021/jp9093172

24. Biesinger MC, Payne BP, Grosvenor AP, Lau LWM, Gerson AR, Smart RSC. Resolving surface chemical states in XPS analysis of first row transition metals, oxides and hydroxides: Cr, Mn, Fe, Co and Ni. *Appl Surf Sci*. 2011;257(7):2717-2730. doi:10.1016/j.apsusc.2010.10.051

25. Bauer FL, Householder AS, Wilkinson JH, Reinsch C. *Handbook for Automatic Computation: Volume II: Linear Algebra*. Springer; 2012.

26. Cottineau T, Rouet A, Fernandez V, Brohan L, Richard-Plouet M. Intermediate band in the gap of photosensitive hybrid gel based on titanium oxide: role of coordinated ligands during photoreduction. *J Mater Chem A*. 2014;2(29):11499-11508. doi:10.1039/C4TA02127D

27. Bagus PS, Nelin CJ, Brundle CR, Chambers SA. A new mechanism for XPS line broadening: the 2p-XPS of Ti(IV). *J Phys Chem C*. 2019;123(13):7705-7716. doi:10.1021/acs.jpcc.8b05576

28. Chambers SA, Sushko PV. Influence of crystalline order and defects on the absolute work functions and electron affinities of TiO_2- and SrO-terminated *n*-SrTiO$_3$(001). *Phys Rev Mater*. 2019;3(12):125803. doi:10.1103/PhysRevMaterials.3.125803